ChemComm
www.rsc.org/chemcomm

In situ transmission electron microscopy investigation of Ce(IV) and Pr(IV) reducibility in a Rh (1%)/$Ce_{0.8}Pr_{0.2}O_{2-x}$ catalyst

C. López-Cartes,[a] S. Bernal,[a] J. J. Calvino,*[a] M. A. Cauqui,[a] G. Blanco,[a] J. A. Pérez-Omil,[a] J. M. Pintado,[a] S. Helveg[b] and P. L. Hansen[b]

[a] *Departamento de Ciencia de los Materiales e Ingeniería Metalúrgica y Química Inorgánica, Universidad de Cádiz, Apdo 40 Puerto Real, 11510- Cádiz, Spain. E-mail: jose.calvino@uca.es; Fax: 34 956 01 6288; Tel: 34 956 01 6333*

[b] *Haldor Topsøe A/S, Nymøllevej 55, DK-2800 Lyngby, Denmark. E-mail: plh@topsoe.dk*

Received (in Cambridge, UK) 26th November 2002, Accepted 28th January 2003
First published as an Advance Article on the web 10th February 2003

***In-situ* Atomic Resolution Transmission Electron Microscopy studies carried out on a Rh/$Ce_{0.8}Pr_{0.2}O_{2-x}$ catalyst, under hydrogen in the temperature range 298–1223 K, show the occurrence of consecutive reduction of Pr^{4+} and Ce^{4+} ions, and the formation of an oxygen-deficient $Ln_{16}O_{30}$ (Ln: Ce, Pr) ordered phase.**

Most of the very important catalytic applications of ceria-based materials are acknowledged to be closely related to their redox properties.[1] Such is the case of three-way catalysis[2] or hydrogen production from partial oxidation of methane.[3]

Recent studies have shown that $CeLnO_{2-x}$[4–7] and $CeLnZrO_{2-x}$[7–9] mixed oxides (Ln: Pr, Tb) exhibit very remarkable redox properties, particularly at low temperature (< 773 K),[2,5,6] thus suggesting highly interesting catalytic applications for these materials.

Compared to the classic ceria and ceria–zirconia systems, the co-existence in these materials of two different reducible cations introduces some additional, very challenging, characterisation problems. A first major question deals with the consecutive or overlapped nature of the two cation reduction processes. Apart from the contribution of XANES,[10] most of the techniques fruitfully applied to the redox characterisation of CeO_2 and CeO_2–ZrO_2[10] cannot, however, provide a conclusive answer to this question. The structural properties of the reduced $CeLnO_{2-x}$ mixed oxides, specifically the likely occurrence of oxygen vacancy ordering phenomena, similar to those exhibited by the binary rare earth oxides: LnO_{2-x} (Ln: Ce, Pr, or Tb),[12] represent a second important question, not clarified as yet.

Here, we report on an *in-situ* High Resolution Transmission Electron Microscopy (HREM) study of this sort of materials. Data concerning a low surface area, 11 $m^2.g^{-1}$, Rh(1%)/$Ce_{0.8}Pr_{0.2}O_{2-x}$ catalyst are presented and discussed. Details of the catalyst preparation procedure are available as complementary information on request. The study was performed on a dedicated microscope, specially designed to apply a wide variety of thermal and chemical treatments inside the instrument.[13,14] The experiments consisted of heating the catalyst step by step at temperatures ranging from 298 to 1223 K, under hydrogen (P_{H_2}: 4 Torr). The HREM images and the Electron Energy Loss Spectroscopy (EELS) data were all recorded under reaction conditions.

Compared to other characterisation techniques, *in situ*-HREM offers the unique possibility of investigating the redox state of both Ce and Pr ions, and the nanostructural features of oxygen vacancy ordering phenomena, simultaneously.

The redox evolution of Ce and Pr ions was investigated by analysing the fine structure in EELS spectra of their $M_{4,5}$ edges. Earlier EELS studies on CeO_2[15] and $Ce_{0.5}Zr_{0.5}O_2$ mixed oxides,[16] have shown that, as the reduction $Ce^{4+}\rightarrow Ce^{3+}$ proceeds, some major changes are observed in the spectrum: a) Both M_4 and M_5 peaks shift down in energy by about 1.4 eV;[15,17] b) There is a damping of the shoulders on the high energy side of the main peaks; c) The intensity ratio: I(M_5)/I(M_4) increases.

No similar *in situ* EELS studies are available for the reduction of Pr-containing oxides. As deduced from Fig. 1, the qualitative evolution of the Pr and Ce $M_{4,5}$ edges shows notable analogies, thus allowing the modifications observed in the Pr spectrum to be interpreted in a similar way as that reported for Ce.

According to Fig. 1, for the catalyst treated in H_2, at 298 K, the position and fine structure features of Ce and Pr spectra are dominated by those corresponding to the Ln^{4+} species.[17,18]

After reduction at 473 K rather abrupt changes are observed in the Pr spectrum: a) A −1.4 eV shift of M_4 and M_5 peaks; b) damping of the shoulders at the higher energy side of these peaks; c) appearance of a small peak at the lower energy side of the M_5 peak. These effects are in good agreement with those reported in XAS studies of the $Pr^{4+}\rightarrow Pr^{3+}$ reduction process.[19,20] Likewise, they are in qualitative agreement with both

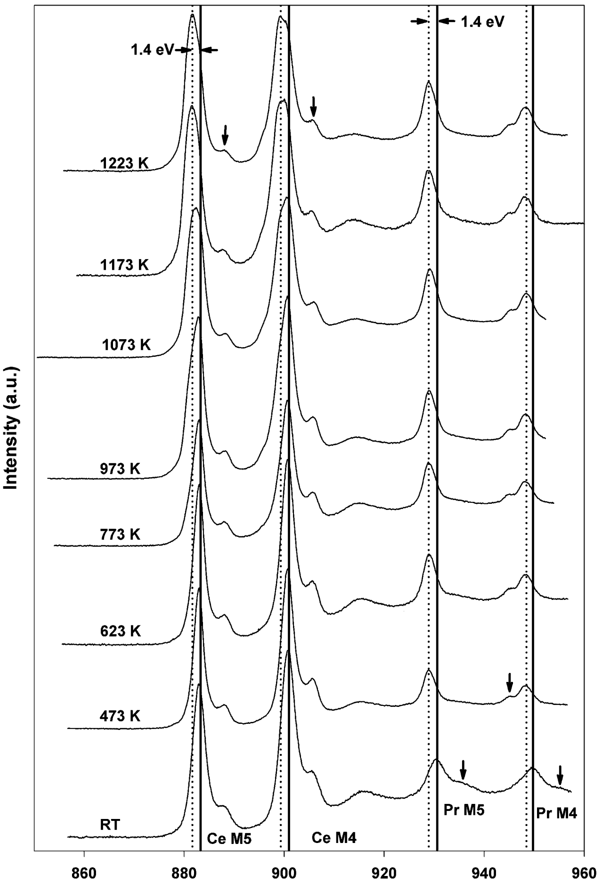

Fig. 1 EELS study of Rh(1%)/$Ce_{0.8}Pr_{0.2}O_{2-x}$ catalyst. Spectra recorded under H_2 pressure (4 mbar) at the indicated temperatures. The peak positions for some of the characteristic features of Ln^{4+} and Ln^{3+} species are marked by the solid and dashed vertical lines respectively.

DOI: 10.1039/b211786j

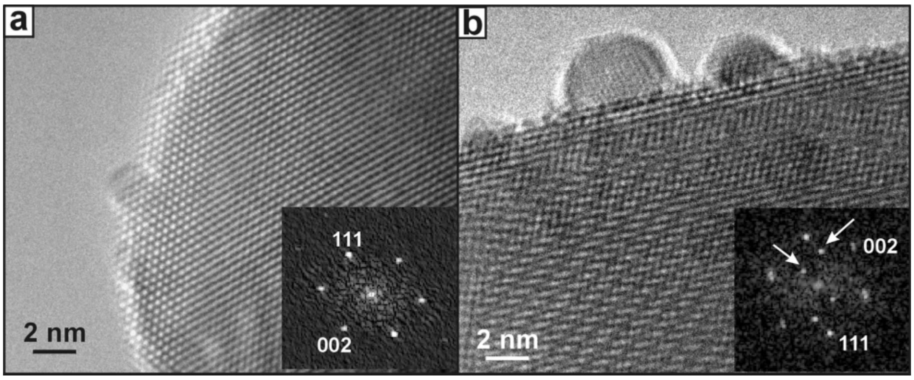

Fig. 2 *In-situ* HREM images recorded on the Rh(1%)/$Ce_{0.8}Pr_{0.2}O_{2-x}$ catalyst: (a) after reduction at 473 K, (b) after reduction at 973 K.

earlier EELS studies[15,17] and our own results, to be commented below, on the cerium reduction. Accordingly, the rather drastic changes occurring in the EELS spectra of Pr are interpreted as due to the $Pr^{4+}\rightarrow Pr^{3+}$ reduction process. Moreover, further increases of the reduction temperature (T_{redn}) have very slight effects on the spectrum, thus indicating that, at 473 K, most of the Pr present in the mixed oxide has already been reduced.

Evidence of Ce^{3+} formation could only be obtained from the spectrum of the catalyst reduced at 973 K, Fig. 1. The lower reducibility of Ce^{4+} is also confirmed by the evolution with T_{redn} of the $I(M_5)/I(M_4)$ ratio, in accordance with which some Ce^{4+} is still present in the sample reduced at 1223 K. We conclude, accordingly, that Pr^{4+} and Ce^{4+} reduction processes take place in a consecutive manner, the disappearance of Pr^{4+} species occurring at much lower temperature.

The *in-situ* TEM technique has also allowed us to investigate how the oxygen vacancies are accommodated into the structure of the mixed oxide. Fig. 2(a) shows an *in-situ* recorded lattice image, which is representative of the catalyst reduced at 473 K. Bidimensional resolution can be clearly appreciated. The Fourier Transform analysis of the fringe pattern shows the existence of 0.312 nm and 0.270 nm lattice spacings. These periodicities are characteristic of the {111} and {200} lattice planes of the oxide fluorite structure. The inset Digital Diffractogram Pattern (DDP) can be assigned to a <110> zone axis of the fluorite.

The first evidence of structural changes in the images could only be obtained upon reduction at 973 K, Fig. 2(b). Besides the {111} and {002} spots, some additional reflections are clearly visible. These extra spots, marked with arrows in the inset DDP, are commensurate with those of the fluorite structure. They may be associated with the long range modulation of the image contrasts. These spots are in fact reflecting a superstructure, which can be indexed on the basis of the fluorite cell as $\frac{1}{4}\{220\}$ and $\{100\} + \frac{1}{4}\{220\}$. The former gives rise to the 0.76 nm modulation observed in this HREM image. The modulation is superimposed to the higher frequency atomic-column contrasts characteristic of <110> fluorite zone axis images. Accordingly, on the catalyst reduced at 973 K, the oxygen vacancies become ordered. No ordering effect could be observed on samples reduced below this threshold temperature.

Accommodation of oxygen vacancies in a homologous series, Ln_nO_{2n-2m}, consisting of superstructures of the fluorite cell, is a well known property of the binary higher 4f oxides.[12] The comparison of the superstructure features observed in Fig. 2(b), with the calculated diffraction patterns reported in ref. 21 for different members of the Ln_nO_{2n-2m} homologous series has allowed us to unambiguously identify in the sample reduced at 973 K the presence of the π-type phase, $Ln_{16}O_{30}$, the least reduced member of the series. These results constitute the first evidence of oxygen vacancy ordering in a Ce–Pr mixed oxide.

As shown here, Pr reduction takes place at temperatures well below the temperature at which vacancy ordering occurs. Full reduction of Pr represents a 20% of the maximum reduction degree attainable by the $Ce_{0.8}Pr_{0.2}O_{2-x}$ mixed oxide. Since the π-phase corresponds to a 25% reduction, some Ce^{3+} must also be present. Our structural observation is thus consistent with the EELS data, in accordance with which cerium reduction starts at 973 K. Further experiments aimed at determining whether temperature and reduction degree are independent factors controlling the onset of the ordering effects are currently underway.

The *in situ* HREM study has been carried out at Haldor Topsøe A/S in Lyngby (Denmark). One of us (C. L. C.) gratefully acknowledges Haldor Topsøe A/S for the financial. Support from the MCYT (Project MAT2002-02782) and the Junta de Andalucía is also acknowledged.

Notes and references

1 A. Trovarelli, *Catal. Rev. Sci. Eng.*, 1996, **38**, 439.
2 M. Shelef and R. W. McCabe, *Catal. Today*, 2000, **62**, 35.
3 L. Pino, V. Recupero, S. Beninati, A. K. Shukla, M. S. Hegde and P. Bera, *Appl. Catal. A: General*, 2002, **225**, 63.
4 M. Y. Sinev, G. W. Graham, L. P. Haack and M. Shelef, *J. Mater. Res.*, 1996, **11**, 1960.
5 S. Bernal, G. Blanco, M. A. Cauqui, P. Corchado, J. M. Pintado and J. M. Rodríguez-Izquierdo, *Chem. Commun.*, 1997, 1545.
6 G. Blanco, J. M. Pintado, S. Bernal, M. A. Cauqui, M. P. Corchado, A. Galtayries, J. Ghijsen, R. Sporken, T. Eickoff and W. Drube, *Surf. Interface Anal.*, 2002, **34**, 120.
7 Z. C. Kang and L. Eyring, *J. Solid State Chem.*, 2000, **155**, 129.
8 A. N. Shigapov, H. W. Jen, G. W. Graham, W. Chun and R. W. McCabe, *Stud. Surf. Sci. Catal.*, 2000, **130**, 1373.
9 S. Rossignol, C. Descorme, C. Kappenstein and D. Duprez, *J. Mater. Chem.*, 2001, **11**, 2587.
10 E. López-Navarrete, A. Caballero, A. R. González-Elipe and M. Ocaña, *J. Mater. Res.*, 2002, **17**, 797.
11 *Catalysis by Ceria and Related Materials*, ed. A. Trovarelli, Imperial College Press, London, 2002.
12 Z. C. Kang and L. Eyring, *Aust. J. Chem*, 1997, **49**, 981.
13 T. W. Hansen, J. B. Wagner, P. L. Hansen, S. Dahl, H. Topsøe and C. J. H. Jacobsen, *Science*, 2001, **294**, 1508.
14 P. L. Hansen, J. B. Wagner, S. Helveg, J. R. Rostrup-Nielsen, B. S. Clausen and H. Topsøe, *Science*, 2002, **295**, 2053.
15 R. Sharma, *Microsc. Microanal.*, 2001, **7**, 494.
16 R. Sharma, *Proceedings of the 52nd SCANDEM*, 2001, 86.
17 T. Manoubi, C. Colliex and P. Rez, *J. Electr. Spectr. and Rel. Phen.*, 1990, **50**, 1.
18 C. C. Ahn and O. L. Krivanek, *EELS Atlas*, 1983.
19 R. C. Karnatak, M. Gasgnier, H. Dexpert, J. M. Esteva, P. E. Caro and L. Albert, *J. Less-Common Met.*, 1985, **110**, 377.
20 R. C. Karnatak, J. M. Esteva, H. Dexpert, M. Gasgnier, P. E. Caro and L. Albert, *Phys. Rev. B*, 1987, **36**(3), 1745.
21 C. López-Cartes, J. A. Pérez-Omil, J. M. Pintado, J. J. Calvino, Z. C. Kang and L. Eyring, *Ultramicroscopy*, 1999, **80**, 19.